

**THE INFLUENCE OF Zn AND Ca ON TENSILE PROPERTIES AND CREEP RESISTANCE OF MgSn6 ALLOY**

In the paper the role of Zn and Ca in enhancement of creep resistance of MgSn6 alloy has been investigated. The influence of zinc on thermal stability of Mg<sub>2</sub>Sn phase has been evaluated as well. Three alloys in as-cast and heat-treated condition have been chosen as a research material – MgSn6, MgSn6Zn1,5 and MgSn6Zn1,5Ca1. The microstructure of investigated alloys has been analysed using the scanning electron microscope, coupled with EDS spectrometer to enable the analysis of chemical composition of individual microstructural constituents. Creep tests have been performed.

It has been revealed, that the microstructure of MgSn6 alloy consists of  $\alpha$ -Mg matrix and  $\alpha$ -Mg+Mg<sub>2</sub>Sn eutectic compound. The addition of Zn caused changes in the morphology of  $\alpha$ -Mg+Mg<sub>2</sub>Sn eutectic compound and formation of Zn-rich phase. Two forms (coarse rod-like primary and lamellar secondary) of CaMgSn phase have been observed in the alloy, containing Ca. It has been found that Zn does not influence the morphology and crystallisation process of Mg<sub>2</sub>Sn phase, which is less thermally stable than CaMgSn phase. Hence, the CaMgSn phase might have a negative influence on creep resistance of MgSn6 alloy. The best creep properties have been exhibited by MgSn6Zn1,5 alloy after age-hardening treatment.

*Keywords:* Magnesium-tin alloys; creep resistance; Mg<sub>2</sub>Sn phase; CaMgSn phase; heat treatment

**Introduction**

Magnesium alloys are the interesting group of modern materials with a great potential for high performance structural applications due to their inherent properties such as low density, high specific strength, superior damping capacity and good castability [1]. On the other hand, one of the crucial factors limiting their wide range of application is their relatively low service temperature. Therefore one of the main directions of development of magnesium alloys is the increase of their high temperature properties, especially creep resistance [2].

The most common way of improving the elevated temperature properties is the formation of thermally stable precipitates or dispersoids along the grain boundaries to resist the deformation by grain boundary sliding. Through the controlled decomposition of a supersaturated solid solution, a fine dispersion of second-phase particles (precipitates) can often be obtained which provides effective obstacles to dislocation motion and hardens the material [3-5]. Notwithstanding, the effectiveness of precipitates at inhibiting basal slip, known as the primary mode of deformation in magnesium below 200°C, depends not only on the mean particle size and number density, but also on the particle shape with the respect to the basal plane, what has been discussed by

Nie [6]. In case of the constant particle size and number density, the most efficient particle morphology for inhibiting basal slip and in the same time enhancing the mechanical properties in ambient temperature and below the temperature of recrystallisation will be that, which is elongated perpendicularly to the basal plane (such as plates and rods formed on the prismatic planes of the matrix), thus maximising the probability that a gliding dislocation will intersect the precipitate. The least efficient particle morphology will be that, which leads to elongation in directions within the basal plane, thus minimizing the probability of a dislocation intersecting the precipitate [3]. On the other hand the precipitates elongated parallelly to the basal plane inhibit the slip of dislocations in prismatic and pyramidal planes, what is important in terms of enhancement of creep resistance.

Due to the low thermal stability of Mg<sub>17</sub>Al<sub>12</sub> phase – the key microstructural constituent of the majority of commercial magnesium alloys and the high costs of rare earth (RE) elements, known to effectively enhance the high temperature properties of magnesium alloys, it is necessary to develop the creep resistant alloys, which do not contain Al and RE as the major alloying elements, but combine the superior high temperature properties of Mg-RE alloys and good castability of Mg-Al alloys. Among many possibilities Mg-Sn and Mg-Ca-Sn systems

<sup>1</sup> SILESIAAN UNIVERSITY OF TECHNOLOGY, INSTITUTE OF MATERIALS ENGINEERING, 8 KRASIŃSKIEGO STR., 40-019 KATOWICE, POLAND

\* Corresponding author: [tomasz.rzychon@polsl.pl](mailto:tomasz.rzychon@polsl.pl)



are of special interests. According to the Mg-Sn binary phase diagram [7-8], the solubility of Sn in  $\alpha$ -Mg solid solution drops sharply from 14,85 wt.% at the eutectic reaction temperature (561°C) to 0,45 wt.% at 200°C, what provides a fundamental basis for improving the mechanical properties of these alloys through ageing. Moreover the thermally stable Mg<sub>2</sub>Sn intermetallic phase has much higher melting point (770°C) than the Mg<sub>17</sub>Al<sub>12</sub> phase (462°C) in Mg-Al alloys, Mg-Sn based alloys are therefore likely to have higher creep resistance at elevated temperatures than Mg-Al based alloys [9]. Sn is also known to increase the corrosion resistance of magnesium and in the same time it presents the better cost effectiveness than rare earth elements. On the other hand some investigation shows the negative influence of Mg<sub>2</sub>Sn phase on the creep resistance of Mg-Sn alloys and reveals its thermal sensitivity [10-11]. Another element, characterised by better cost effectiveness than rare earth elements is calcium. It has been reported, that Ca forms thermally stable intermetallic particles in the matrix, enhancing the creep strength. The improvement of this property was achieved with the increasing Ca content and was attributed to the diminishing of the less stable Mg<sub>2</sub>Sn particles and formation of the more thermally stable CaMgSn phase which strengthens both matrix and grain boundaries during creep deformation [12-13]. Kainer et al. have reported that ternary CaMgSn phase not only shows high thermal stability up to 500°C, but observed, that the alloys containing CaMgSn phase show favorable creep resistance also in compressive mode [1,14-15].

The main aim of the present work is evaluation of the influence of Zn and Ca on creep resistance of magnesium-tin alloys, as well as verification of previous research, reporting the enhanced creep properties of magnesium-tin alloys, containing this elements.

## 1. Experimental methods

Three different Mg-Sn alloys, with chemical compositions given in TABLE 1 have been selected as a research material in order to investigate the influence of Zn and Ca on microstructure and creep properties of MgSn6 alloy. Zn is known to impart the dispersion of Mg<sub>2</sub>Sn phase [16-18]. The mentioned effect of Zn addition might has a beneficial influence on creep resistance of MgSn6 alloy by the decrease of mean particle spacing  $\lambda$  and altering the particle shape with the respect to the basal plane. The addition of Ca should result in formation of CaMgSn phase, characterised by the better thermal stability than Mg<sub>2</sub>Sn phase [14-15].

TABLE 1

Chemical compositions of investigated alloys (wt.%)

	Mg	Sn	Zn	Ca
MgSn6	93.98	6.02	—	—
MgSn6Zn1,5	92.71	5.95	1.34	—
MgSn6Zn1,5Ca1	91.27	6.05	1.48	1.20

The investigated alloys were fabricated in alumina crucibles using a vacuum induction furnace. 99,6 wt.% purity Mg, Sn, Zn and Mg-10Ca master alloy were used as the starting materials in production of the experimental alloys. Before the melting process the furnace chamber was flushed with Ar to remove the residues of oxygen and to eliminate the possibilities of oxidation and contamination of the melt. The process was conducted in Ar protective atmosphere under the pressure of 650 Tr to reduce the evaporation of the alloys constituents. The temperature was set to 720°C. Before the casting process the melt had been electro-dynamically stirred for 3 minutes, using the eddy currents and enabling its homogenisation. The experimental alloys ingots were casted to the quartz sand casting moulds.

The investigated samples were obtained from central part of the ingots. The specimens were prepared for investigation following the Struers specimen preparation system (grinding on abrasive papers with grit from 120 to 1200 and polishing on polishing cloths using the polycrystalline diamond water suspensions with grain size from 6  $\mu$ m to 0,25  $\mu$ m; the Struers OP-AN solution of 0,05  $\mu$ m Al<sub>2</sub>O<sub>3</sub> was used for the final polishing of the specimens). Due to the relatively fast oxidation of the specimens during the final polishing the cloth was systematically moisturised with 99,8% purity ethanol.

The analysis of microstructure were carried out on the Hitachi S-3400N scanning electron microscope. Photomicrographs were registered using the imaging technique with a detection of backscattered secondary electrons (BSE). Chemical composition analysis were done using Thermo NORAN System 7 X-Ray EDS detector coupled with the scanning electron microscope, with an accelerating voltage of 15 kV in a high vacuum. The phase composition analysis were carried out on the X'Pert<sup>3</sup> Powder X-Ray diffractometer, equipped with the cooper anode lamp ( $\lambda_{\text{CuK}\alpha} = 1,5406 \text{ \AA}$ ,  $I = 30 \text{ mA}$ ,  $U = 40 \text{ kV}$ ). PiXcel 1D strip detector with monochromator was used. The registration of X-Ray was conducted in the angular range of  $2\theta$  from 10° to 90° with the step of 0,02°. The bulk samples were applied. The detected phases have been identified basing on the International Centre for Diffraction Data database. The static tensile tests were performed on Zwick/Roell Kappa 50DS tester. Tensile strength, yield strength and percentage elongation at break were determined. The creep tests were conducted using the Zwick/Roell Kappa 50DS electromechanical creep tester under a constant load. The heating rate was set to 5°C/min., temperature to 180±3°C and time to 110 h. The strain was measured with the first accuracy class extensometer. The parameters (force, time, temperature and elongation) were registered using Test X'Pert 2 software.

## 2. Results and discussion

### 2.1. Microstructure of investigated alloys in as-cast condition and after age-hardening treatment

The microstructural investigation of as-cast MgSn6 alloy have shown the existence of the matrix dendrites and lamellar

eutectic compound located in the interdendritic areas. The EDS chemical composition analysis and X-ray diffraction analysis revealed that the matrix is a solid solution of around 1 at.% of Sn in  $\alpha$ -Mg (Fig. 1, TABLE 2, pt. 3), whilst the eutectic compound is composed of  $\alpha$ -Mg and  $Mg_2Sn$  phases (Fig. 1, TABLE 2, pts. 1-2). Additionally, SEM investigation revealed the segregation of tin in the dendrites of the  $\alpha$ -Mg (darker areas of matrix are Sn-poor, lighter areas are Sn-rich, Fig. 1).

The addition of Zn ( $MgSn6Zn1,5$  alloy) affects the morphology the  $\alpha$ -Mg+ $Mg_2Sn$  eutectic. In case the alloy without Zn the lamellar  $\alpha$ -Mg+ $Mg_2Sn$  eutectic is observed in the interdendritic regions (Fig. 1), whereas in the alloy with zinc morphology of  $Mg_2Sn$  is rather massive (Fig. 2, TABLE 3, pt. 1). The similar influence of Zn on the morphology of  $\alpha$ -Mg+ $Mg_2Sn$  eutectic compound have been reported previously by Cheng et al. [19] and Bamberger [20]. In the vicinity of  $\alpha$ -Mg+ $Mg_2Sn$  eutectic

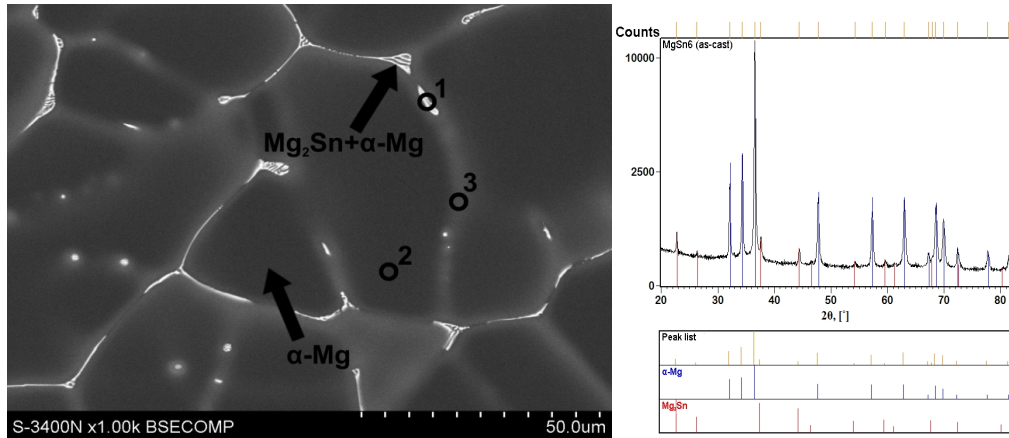


Fig. 1. SEM image and X-ray diffraction pattern of as-cast  $MgSn6$  alloy

TABLE 2

Results of EDS quantitative chemical composition analysis obtained from points indicated in Fig. 1 (at.%)

	Mg	Sn
Point 1	77.3	22.7
Point 2	99.0	1.0
Point 3	96.2	3.8

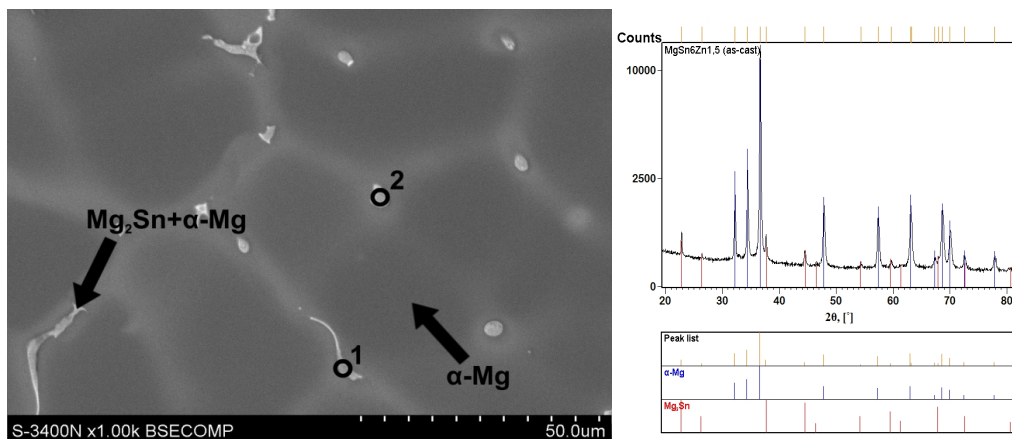


Fig. 2. SEM image and X-ray diffraction pattern of as-cast  $MgSn6Zn1,5$

TABLE 3

Results of EDS quantitative chemical composition analysis obtained from points indicated in Fig. 2 (at.%)

	Mg	Sn	Zn
Point 1	69.8	29.2	1.0
Point 2	62.0	1.1	36.9
Point 3	98.9	1.1	-
Point 4	93.6	1.9	4.5

the phase rich in Zn (Fig. 2, TABLE 3, pt. 2) has been observed. Due to the low content, identification of this compound by X-ray diffraction analysis have not been possible. However, Zn-rich phases with similar morphology identified as MgZn phase have been observed in alloys with higher zinc content (>3%) [20]. The local increase of Zn and Sn in the vicinity of interdendritic areas have been also observed (Fig. 2, TABLE 3, pts. 3-4).

In MgSn6Zn1,5Ca1 alloy the coarse rod-like precipitates consisting of Mg, Sn and Ca and lamellar compound with the same chemical composition have been observed. These intermetallic compounds have been located in the grain interiors and interdendritic regions. Basing on the X-ray diffraction analysis, EDS chemical composition analysis and the literature studies

[1,15,21] it could be found that the coarse rod-like precipitates are the primary CaMgSn phase particles (Fig. 3, TABLE 4, pt. 1) formed in the beginning stage of the solidification process, whilst the presence of lamellar eutectic compound (Fig. 3, TABLE 4, pt. 2) results from the secondary formation of CaMgSn phase in  $L \rightarrow (Mg) + Ca_{2-x}Mg_xSn + Mg_2Sn$  reaction simultaneously with  $Mg_2Sn$  phase (Fig. 3, TABLE 4, pt. 3) [1].

The influence of heat treatment on microstructure of investigated alloys has been evaluated. The parameters have been selected experimentally, depending on the peak hardness of the alloy and are presented in TABLE 5. The selected parameters of solution treatment ensured a complete dissolution of  $Mg_2Sn$  phase (Fig. 4) in all investigated alloys. In case of

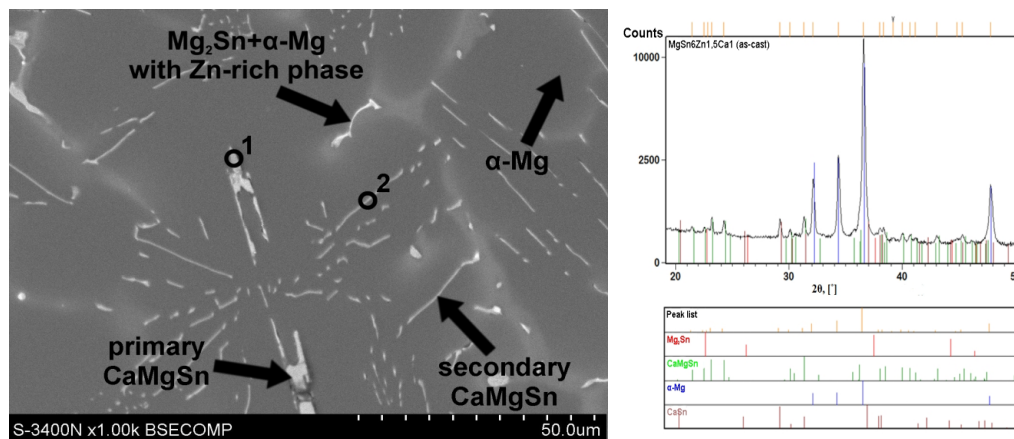


Fig. 3. SEM image and X-ray diffraction pattern of as-cast MgSn6Zn1,5Ca1

TABLE 4

Results of EDS quantitative chemical composition analysis obtained from points indicated in Fig. 3 (at.%)

	Mg	Sn	Zn	Ca
Point 1	47.2	30.0	—	22.8
Point 2	82.5	11.9	0.8	4.8

TABLE 5

Parameters of heat treatment of investigated alloys

	Solution treatment	Ageing treatment
MgSn6	4h/520°C, water quenching	48 h/250°C, water quenching
MgSn6Zn1,5	4h/520°C, water quenching	72 h/250°C, water quenching
MgSn6Zn1,5Ca1	4h/520°C, water quenching	120 h/250°C, water quenching

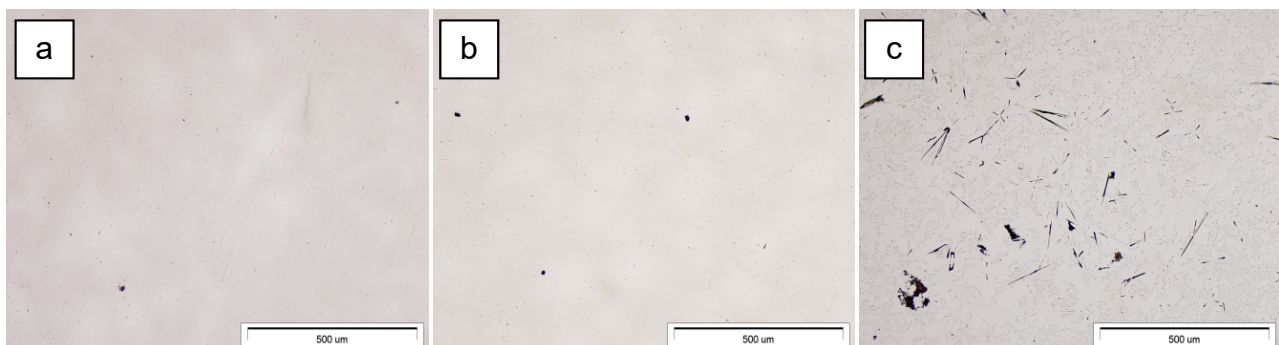


Fig. 4. Microstructure of investigated alloys after solution treatment of 4h/520°C (a – MgSn6, b – MgSn6Zn1,5, c – MgSn6Zn1,5Ca1)

MgSn6Zn1,5Ca1 alloy undissolved residues of primary and secondary CaMgSn phase have been observed, even after solution treatment of 8h/520°C.

The applied age hardening treatment has led to precipitation of significant amount of needle-like and plate-like precipitates of Mg<sub>2</sub>Sn phase in all investigated alloys (Fig. 5). The Mg<sub>2</sub>Sn precipitates have been observed in grain interiors, nevertheless more massive precipitates of Mg<sub>2</sub>Sn phase (Fig. 5.1a, 5.2a, 5.3a) have been recognised on the grain boundaries. Considering complete dissolution of Mg<sub>2</sub>Sn phase after the solution treatment (Fig. 4), the source of their presence is probably their secondary formation during the heat treatment in the areas enriched in Sn, as a result of microsegregation in  $\alpha$ -Mg dendrites, as well as the coagulation of disperse precipitates in this region. It has been discovered, that zinc has no influence on the direction of

precipitates growth, since the Mg<sub>2</sub>Sn dispersoids have been observed both on basal and prismatic planes of  $\alpha$ -Mg matrix (the precipitates have been observed in all directions, regardless to the zinc content). Nevertheless the increase of precipitates number has been revealed in MgSn6Zn1,5 alloy, what might be attributed to increased zinc content, comparing to the basal MgSn6 alloy and the presence of Zn-rich phase, occurring simultaneously with Mg<sub>2</sub>Sn phase [3]. In case of MgSn6Zn1,5Ca1 alloy the decrease of the volume fraction of Mg<sub>2</sub>Sn phase precipitates has been found, according to the effect of tin consumption during the formation process of CaMgSn phase [12-13]. Furthermore the microstructural investigation confirmed the higher thermal stability of CaMgSn phase comparing to Mg<sub>2</sub>Sn phase due to the lack of solubility of both primary and secondary CaMgSn phase during the heat treatment.

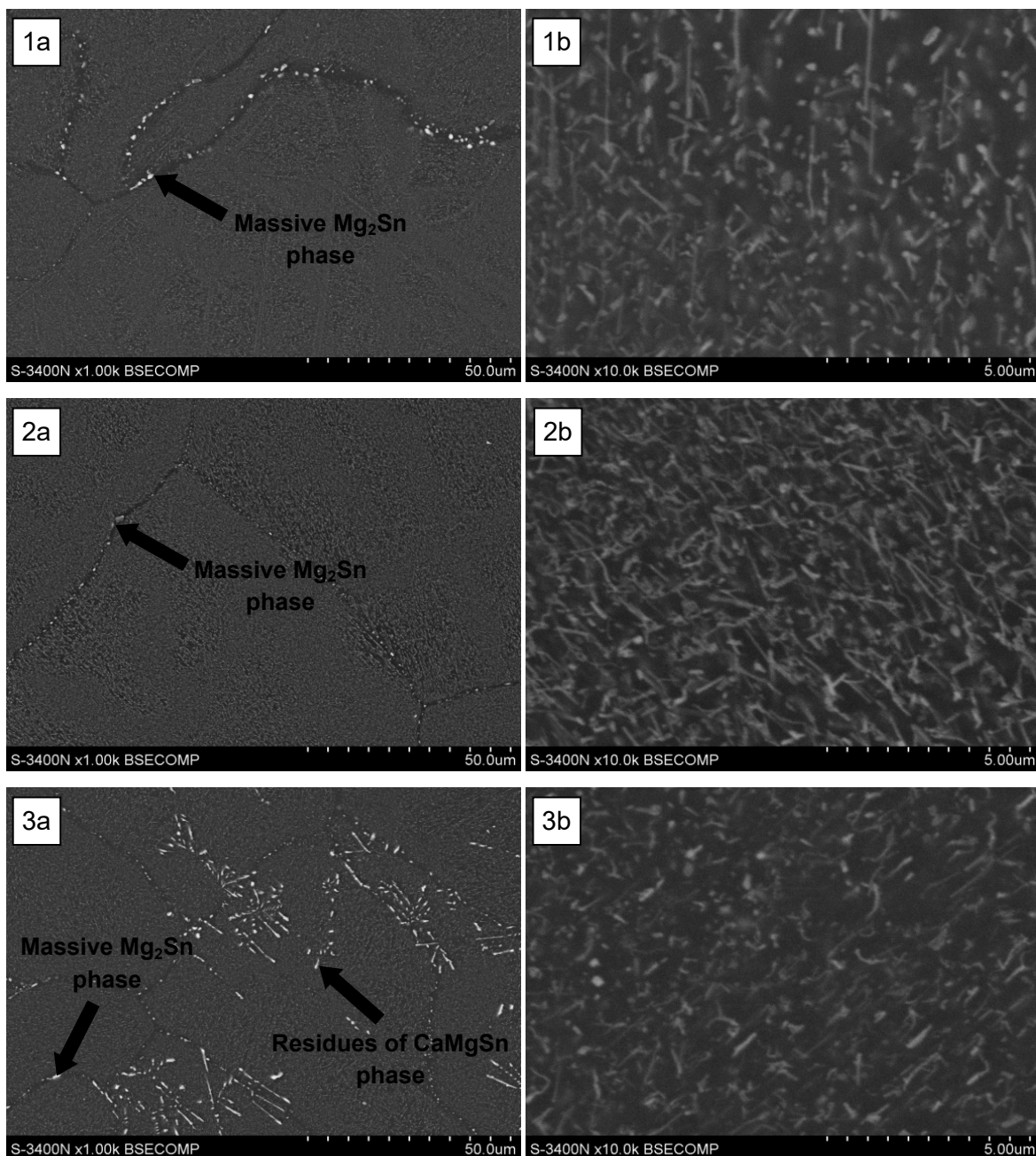


Fig. 5. SEM images of investigated alloys after age-hardening treatment (5.1 – MgSn6 alloy, 5.2 – MgSn6Zn1,5 alloy, 5.3 – MgSn6Zn1,5Ca1 alloy)

## 2.2. Mechanical and creep properties of as-cast and heat-treated alloys

The results of mechanical properties investigation (TABLE 6) show the increase of tensile strength and yield strength in case of MgSn6 and MgSn6Zn1,5 alloys after age-hardening treatment as a result of the precipitation of the Mg<sub>2</sub>Sn phase. The MgSn6Zn1,5 alloy exhibited the best tensile properties due to beneficial effect of Zn on increasing the number of fine precipitates of Mg<sub>2</sub>Sn phase, that are effective obstacles in dislocation motion during the plastic deformation of the alloy. High tensile properties of Zn containing alloy have been obtained and explained by Sasaki et al. and Son et al. [17-18,23-24]. No explanation for the high value of elongation (17.1%), observed in the as-cast MgSn6Zn1,5 alloy has been found, nevertheless it has decreased to 7.1% after applied age-hardening treatment. On the contrary to the research of Kim et al. [1], the decrease of tensile properties of MgSn6Zn1,5Ca1 alloy after age-hardening treat-

ment has been observed. The reason of mechanical properties deterioration may be the coarse morphology of CaMgSn phase, which sharp edges are potential sources of material cracking during deformation process.

Likewise in case of mechanical properties, the increase of creep resistance in case of heat treated MgSn6 and MgSn6Zn1,5 alloys, comparing to as-cast alloys have been found (Fig. 6, TABLE 7). It could be attributed to the formation of Mg<sub>2</sub>Sn disperse precipitates [9]. Basing on the Nie's theory [6] it can be concluded, that the disperse precipitates of Mg<sub>2</sub>Sn phase, observed in all heat treated alloys are effective obstacles in dislocation motion, that is the primary creep deformation mode of magnesium alloys. Furthermore, better creep resistance has been exhibited by the alloy containing Zn addition (MgSn6Zn1,5) than in case of MgSn6 alloy. Even heat-treated MgSn6 alloy, without Zn addition is characterised by the lower creep resistance than as-cast MgSn6Zn1,5 alloy. An additional increase of this property have been noticed in MgSn6Zn1,5 alloy after age-hardening treatment, classifying it as the best of all investigated alloys in terms of creep resistance. According to the Orowan's mechanism, the increase of the volume fraction of Mg<sub>2</sub>Sn disperse precipitates after addition of Zn, resulting also in the decrease of mean particle spacing  $\lambda$  leads to enhancement of creep resistance of Mg-Sn alloys containing Zn. Although the creep resistance of as-cast MgSn6Zn1,5Ca1 alloy was better than the creep resistance of as-cast MgSn6 alloy it has been considered as the worst of all investigated alloys. Despite of the higher thermal stability of CaMgSn phase the creep resistance of Ca containing alloy has decreased after the heat treatment. This decrease may be justified by the consumption of tin in

TABLE 6

Mechanical properties of investigated alloys  
(T6 represents the alloy after age-hardening treatment)

	UTS, [MPa]	YTS, [MPa]	EI, [%]
MgSn6	87	41	3.4
MgSn6(T6)	127	66	3.5
MgSn6Zn1,5	171	50	17.1
MgSn6Zn1,5(T6)	193	92	7.1
MgSn6Zn1,5Ca1	118	65	3.4
MgSn6Zn1,5Ca1(T6)	102	61	2.0

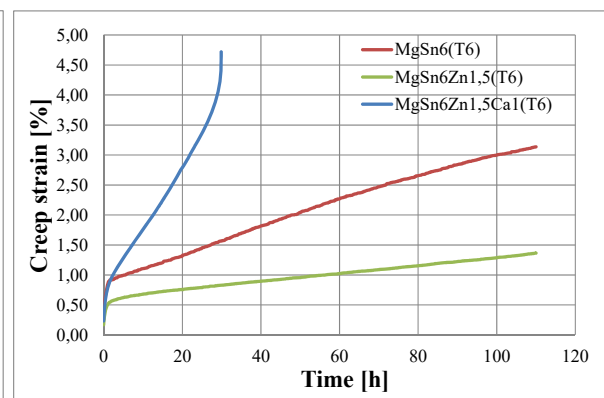
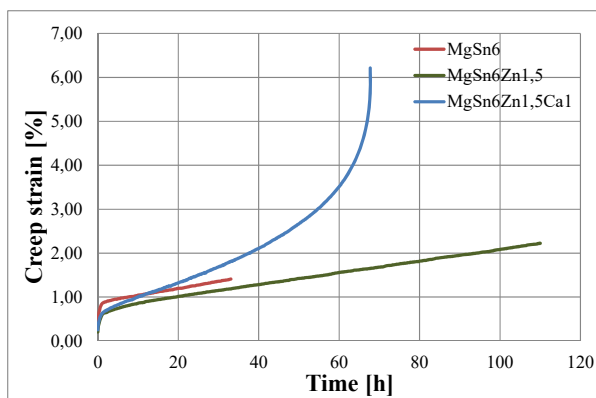


Fig. 6. Creep curves obtained during the creep tests of investigated alloys; (T6) represents the alloys after age-hardening treatment

TABLE 7

Results of creep tests of investigated alloys (T6 – age-hardening treatment)

	$\sigma$ , [MPa]	T, [°C]	$\epsilon_c$ , [%]	$\dot{\epsilon}$ , [s <sup>-1</sup> ]	t, [h]	$\epsilon_p$ , [%]
MgSn6	30	180	1.4	$4.4 \times 10^{-08}$	33.1	0.34
MgSn6(T6)	30	180	3.1	$6.3 \times 10^{-08}$	110.0	0.27
MgSn6Zn1,5	30	180	2.2	$3.7 \times 10^{-08}$	110.0	0.21
MgSn6Zn1,5(T6)	30	180	1.4	$3.4 \times 10^{-08}$	110.0	0.17
MgSn6Zn1,5Ca1	30	180	6.2	$9.9 \times 10^{-08}$	67.7	0.26
MgSn6Zn1,5Ca1(T6)	30	180	4.7	$2.8 \times 10^{-07}$	29.9	0.24

the formation process of CaMgSn phase and in the same time diminish of Mg<sub>2</sub>Sn phase precipitates. The observed influence of Ca addition on creep resistance is reverse to that, presented by Nayyeri and Mahmudi [12-13], what has been attributed to the morphology of CaMgSn phase, observed in investigated MgSn<sub>6</sub>Zn<sub>1.5</sub>Ca<sub>1</sub> alloy. The coarse rod-like precipitates of primary CaMgSn phase are the sources of material decohesion. The differences in thermal expansivity of  $\alpha$ -Mg matrix and CaMgSn phase leads to microcracking of material in the vicinity of phase interfaces and sharp edges of CaMgSn phase and simultaneous decrease of creep resistance of the alloy. Hence the positive role of coarse precipitates of CaMgSn phase in enhancement of creep resistance of Mg-Sn alloys is questionable.

### 3. Conclusions

- The microstructure of magnesium-tin alloys consists of  $\alpha$ -Mg matrix and  $\alpha$ -Mg-Mg<sub>2</sub>Sn eutectic compound, located mainly on the grain boundaries. The addition of zinc results in transformation of  $\alpha$ -Mg-Mg<sub>2</sub>Sn eutectic compound to deformed form and formation of Zn-rich phase, occurring simultaneously with Mg<sub>2</sub>Sn phase. In case of Ca addition the new CaMgSn phase is formed in grains interiors and interdendritic regions with simultaneous diminish of Mg<sub>2</sub>Sn phase. Two forms of CaMgSn phase have been recognised – coarse rod-like primary CaMgSn and lamellar secondary CaMgSn. Microsegregation of tin and zinc in  $\alpha$ -Mg dendrites has been revealed.
- The age-hardening treatment resulted in precipitation of disperse needle-like and plate-like precipitates of Mg<sub>2</sub>Sn phase in grain interiors. More massive precipitates have been observed in the vicinity of grain boundaries, enriched in tin as a result of microsegregation of this element. No influence of Zn on the direction of Mg<sub>2</sub>Sn precipitates growth has been identified. However, in alloy containing Zn an increased number of dispersoids has been observed. It has been revealed that CaMgSn phase is characterised by the better thermal stability than Mg<sub>2</sub>Sn phase, due to the fact, that both primary and secondary CaMgSn phase have been not dissolved during the heat treatment.
- It has been concluded, that the presence of disperse precipitates of Mg<sub>2</sub>Sn phase enhances the tensile properties and creep resistance of Mg-Sn alloys, especially in Zn containing alloy, what confirms a beneficial influence of this element on Mg<sub>2</sub>Sn phase. However, the negative influence of CaMgSn phase on tensile and creep properties of Mg-Sn alloy has been discovered, what has been attributed to the coarse morphology of mentioned phase, leading to material decohesion in the vicinity of phase interfaces, caused by the differences in thermal expansivity between  $\alpha$ -Mg matrix and CaMgSn phase.

### Acknowledgments

The present work was supported by the Polish Ministry of Science and Higher Education under the strategical project No. POIG.01.01.02-00-015/09 (FSB-71/RM3/2010). The author is grateful to the following persons: MSc. Adam Gryc for participation in the preparation of the manuscript and Ph.D Bartosz Chmiela for research with the use of the SEM.

### REFERENCES

- [1] D.H Kim, J.Y. Lee, H.K. Lim, J.S. Kyeong, W.T. Kim, D.H. Kim, The Effect of Microstructure Evolution on the Elevated Temperature Mechanical Properties in Mg-Sn-Ca System. *Materials Transactions* **49**, 10, 2405-2413 (2008).
- [2] B.L. Mordike, T. Ebert, Magnesium. Properties – applications – potential. *Materials Science and Engineering A* **302**, 37-45 (2001).
- [3] C.L. Mendis, C.J. Bettles, M.A. Gibson, C.R. Hutchinson, An enhanced age hardening response in Mg-Sn based alloys containing Zn. *Materials Science and Engineering A* **435-436**, 163-171 (2006).
- [4] C.L. Mendis, C.J. Bettles, M.A. Gibson, C.R. Hutchinson, Refinement of precipitate distributions in an age-hardenable Mg-Sn alloy through microalloying. *Philosophical Magazine Letters* **86**, 7, 443-456 (2006).
- [5] E. Orowan, Symposium on Internal Stresses in Metals and Alloys. Session III Discussion Institute of Metals, London, 1948, p. 451.
- [6] J.F. Nie, Effects of precipitate shape and orientation on dispersion strengthening in magnesium alloys. *Scripta Materialia* **48**, 1009-1015 (2003).
- [7] A.A. Nayeb-Hashemi, J.B. Clark, The Mg-Sn (Magnesium-Tin) system. *Bulletin of Alloy Phase Diagrams* **5**, 5, 466-476 (1984).
- [8] T.B. Massalski, *Binary Alloy Phase Diagrams*. ASM International, (1990).
- [9] H. Liu, Y. Chen, Y. Tang, S. Wei, G. Niu, The microstructure, tensile properties, and creep behavior of as-cast Mg-(1-10)%Sn alloys. *Journal of Alloys and Compounds* **440**, 122-126 (2007).
- [10] K. Suresh, K.P. Rao, Y.V.R.K. Prasad, N. Hort, K.U. Kainer, Microstructure and mechanical properties of as-cast Mg-Sn-Ca alloys and effect of alloying elements. *Transactions of Nonferrous Metals Society of China* **23**, 3604-3610 (2013).
- [11] T. Abu Leil, N. Hort, W. Dietzel, C. Blawert, Y. Huang, K.U. Kainer, K.P. Rao, Microstructure and corrosion behavior of Mg-Sn-Ca alloys after extrusion. *Transactions of Nonferrous Metals Society of China* **19**, 1, 40-44, (2009).
- [12] G. Nayyeri, R. Mahmudi, The microstructure and impression creep behavior of cast, Mg-5Sn-xCa alloys. *Materials Science and Engineering A* **527**, 2087-2098 (2010).
- [13] G. Nayyeri, R. Mahmudi, Effects of Ca additions on the microstructural stability and mechanical properties of Mg-5%Sn alloy. *Materials and Design* **32**, 1571-1576 (2011).
- [14] T. Abu Leil, Y. Huang, H. Dieringa, N. Hort, K.U. Kainer, J. Bursik, Y. Jiraskova, K.P. Rao, Effect of heat treatment on the microstructure and creep behavior of Mg-Sn-Ca Alloys. *Materials Science Forum* **546**, 69-72 (2007).

- [15] A. Kozlov, M. Ohno, R. Arroyave, Z.K. Liu, Schmid-Fetzer Phase equilibria, thermodynamics and solidification microstructures of Mg–Sn–Ca alloys. Part 1: Experimental investigation and thermodynamic modeling of the ternary Mg–Sn–Ca system. *Intermetallics* **16**, 299-315 (2008).
- [16] C.L. Mendis, C.J. Bettles, M.A. Gibson, C.R. Hutchinson, An enhanced age hardening response in Mg–Sn based alloys containing Zn. *Materials Science and Engineering A* **435-436**, 163-171 (2006).
- [17] T.T. Sasaki, K. Oh-ishi, T. Ohkubo, K. Hono, Enhanced age hardening response by the addition of Zn in Mg–Sn alloys. *Scripta Materialia* **55**, 251-254 (2006).
- [18] T.T. Sasaki, K. Oh-ishi, T. Ohkubo, K. Hono, Effect of double aging and microalloying on the age hardening behavior of a Mg–Sn–Zn alloy. *Materials Science and Engineering A* **530**, 1-8 (2011).
- [19] W.L. Cheng, S.S. Park, W.N. Tang, B.S. You, B.H. Koo, Influence of alloying elements on microstructure and microhardness of Mg–Sn–Zn-based alloys. *Transactions of Nonferrous Metals Society of China* **20**, 2246-2252 (2010).
- [20] M. Bamberger, Phase formation in Mg–Sn–Zn alloys – thermodynamic calculations vs experimental verification. *Journal of Materials Science* **41**, 2821-2829 (2006).
- [21] M. Keyvani, R. Mahmudi, G. Nayyeri, Effect of Bi, Sb, and Ca additions on the hot hardness and microstructure of cast Mg–5Sn alloy. *Materials Science and Engineering A* **527**, 7714-7718 (2010).
- [23] T.T. Sasaki, J.D. Ju Hono, K.K.S. Shin, Heat-treatable Mg–Sn–Zn wrought alloy. *Scripta Materialia* **61**, 80-83 (2009).
- [24] H. Son, J. Lee, H. Jeong, T.J. Konno, Effects of Al and Zn additions on mechanical properties and precipitation behaviors of Mg–Sn alloy system. *Materials Letters* **65**, 1966-1969 (2011).